Steady-State Analysis of Continuous Adaptation in Acoustic Feedback Reduction Systems for Hearing-Aids

Marcio G. Siqueira, *Member, IEEE,* and Abeer Alwan, *Member, IEEE*

***Abstract*—Acoustic feedback is a problem in hearing aids that contain a substantial amount of gain, hearing aids that are used in conjunction with vented or open molds, and in-the-ear hearing aids. Acoustic feedback is both annoying and reduces the maximum usable gain of hearing-aid devices. This paper studies analytically the steady-state convergence behavior of LMS-based adaptive algorithms when used in continuous adaptation to reduce acoustic feedback. A bias is found in the adaptive filter's estimate of the hearing-aid acoustic feedback path. Methods for reducing this bias and producing an improved estimate of the acoustic feedback path are analyzed and compared. It is shown that by the use of a delay in the forward or cancellation paths of the hearing aid plant, and for representative feedback paths, it is possible to reduce this bias by more than 15 dB.**

***Index Terms*—Adaptive filters, feedback, hearing aids.**

I. Introduction

A MAJOR complaint of hearing-aid users is acoustic feedback which is perceived as whistling or howling (at oscillation) or distortion (at sub-oscillatory intervals). This feedback occurs, typically at high gains, because of leakage from the receiver to the microphone (Fig. 1).

Acoustic feedback suppression in hearing-aids is important since it can increase the maximum insertion gain of the aid. The ability to achieve target insertion gain leads to better utilization of the speech bandwidth and, hence, improved speech intelligibility for the hearing-aid user. The acoustic path transfer function can vary significantly depending on the acoustic environment [1]. Hence, effective acoustic feedback cancellers must be adaptive.

Continuous and noncontinuous adaptation systems for feedback reduction have been proposed in the past. Non-continuous adaptation systems periodically use a training sequence, such as white noise, at the output of the hearing aid for adaptation of the feedback canceller coefficients. The interference nature of this training sequence, however, reduces the signal-to-noise ratio (SNR) and thus is only useful for the profoundly deaf who would not be affected by the noise sequence. Kates [2] proposes such a system that adapts to the cancellation path when howling is detected. Maxwell and Zurek [3] also propose a noncontinuous adaptation system that adjusts the adaptive filter coefficients only when the input signal level is low. Both systems may be objectionable because they limit adaptation to only when silent or howling intervals are detected.

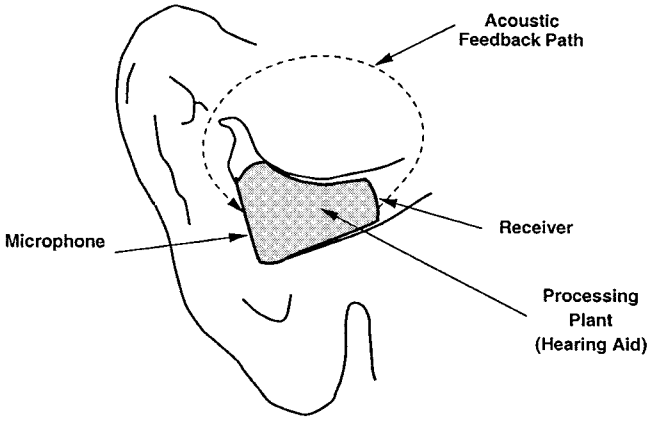

Fig. 1. Acoustic feedback in a hearing aid inside of a human ear.

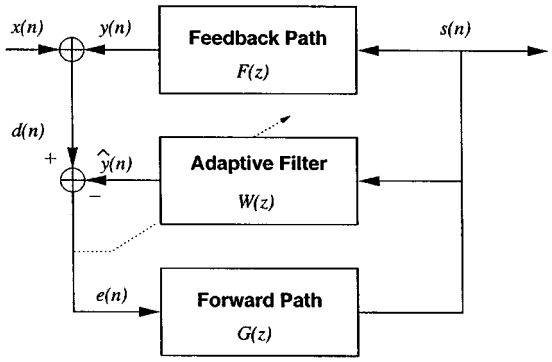

Fig. 2. Hearing aid plant with an adaptive filter for performing continuous feedback reduction. $G(z)$ is the processing plant transfer function and $F(z)$ is the electroacoustic feedback path.

Continuous adaptation systems are, therefore, preferred. They constantly adapt the filter coefficients based on the input signal, and do not require any type of training sequence, as shown in Fig. 2. In this figure, the adaptive filter $W(z)$ attempts to continuously estimate the feedback path transfer function $F(z)$. The main disadvantage of continuous adaptation systems is that the response signal $d(n)$ is the addition of the feedback signal $y(n)$ and the plant input signal $x(n)$, which are correlated, causing the hearing aid output $s(n)$ to be correlated with $x(n)$ and, hence, an adaptive filter cannot properly estimate the feedback path. Delays have been proposed ([1], [3], [4]) to

Manuscript received September 25, 1997; revised July 26, 1999. This work was supported in part by NIH. The associate editor coordinating the review of this manuscript and approving it for publication was Dr. Dennis R. Morgan.

The authors are with the Speech Processing and Auditory Perception Laboratory, Department of Electrical Engineering, University of California, Los Angeles, CA 90095-1594 USA (e-mail: alwan@icsl.ucla.edu).

Publisher Item Identifier S 1063-6676(00)05179-8.

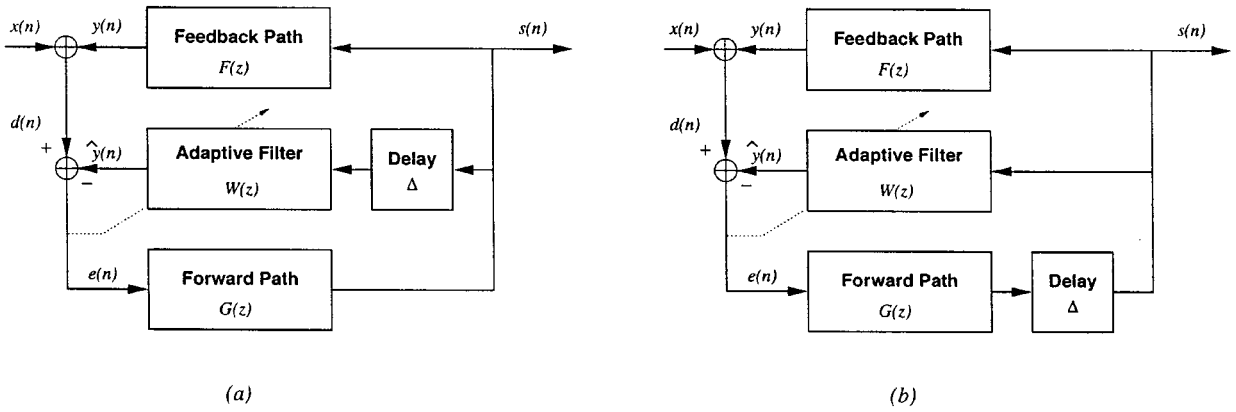

Fig. 3. Model of the hearing aid plant with (a) delay in the cancellation path and (b) delay in the forward path.

decorrelate the input signal $x(n)$ from the input to the adaptive filter $s(n)$. Bustamante *et al.* [1], who were the first to propose a continuous adaptation system that used an LMS-based adaptive filter [Fig. 3(a)], indicate that a delay of 1 ms placed in the cancellation path is sufficient for decorrelating speech signals. However, they do not present a mathematical justification for their choice of delay.

Estermann and Kaelin [4] use a frequency-domain approach for reducing the complexity of continuous adaptation systems. The main difference between Estermann and Kaelin's system and the ones used by Bustamante *et al.* [1] and by Maxwell and Zurek [3] is that the delay is placed in the forward path, as shown in Fig. 3(b). Again, Estermann and Kaelin chose the delay in the forward path by real-time (DSP) evaluation with no analytical justification.

Besides the use of a delay, other techniques such as spectrum compression [5] have been proposed to decorrelate $x(n)$ and $s(n)$.

This paper is a first step toward an analytical approach for evaluating the performance of adaptive filters when correlated inputs are used in continuous adaptation systems. We present a mathematical analysis of the steady-state performance and show that when the input signal to the continuous-adaptation hearing aid plant $[x(n)]$ is correlated, a bias is introduced in the adaptive filter taps' estimate, causing nonoptimal feedback cancellation. It should be noted that most adaptive filtering applications do not present a bias in the taps' solution. In fact, for other applications, such as echo cancellation and channel equalization, it is possible to prove that the mean of the taps of adaptive algorithms, such as the least mean squares (LMS) algorithm [6], converges to the optimal solution for appropriate choices of the convergence factor, independent of the input signal characteristics [7].

The use of delays in the forward and cancellation paths of a hearing-aid plant, as suggested previously by Bustamante *et al.* [1] and Estermann and Kaelin [4], is analytically shown here to reduce the bias when the input signal is correlated. System analysis for the cases where delays are used in the forward and cancellation paths are then studied when the input signal $x(n)$ is an Mth-order Markov Process. This paper will also show, among other results, that the use of a forward path delay results in a bias that is independent of the feedback path transfer function, and that the same result does not hold for a delayed cancellation path.

II. Hearing-Aid Model

In most digital hearing-aids, the processing plant consists of an automatic gain control (AGC) to limit the dynamic range of the input signal, a frequency-shaping filter that correlates with the subjects' audiogram, and a user-adjusted gain control system. For simplicity, the hearing-aid forward path $G(z)$ in Fig. 2 is modeled as $G(z) = G_0 z^{-1}$ [4] without an AGC mechanism or a frequency-shaping filter.

The acoustic feedback path of a hearing-aid accounts for the leakage of sound from the hearing-aid receiver in the ear canal, through and around the hearing-aid earmold, to the hearing-aid microphone. The acoustic feedback path also includes the responses of the hearing-aid microphone and receiver. The acoustic feedback path model, $F(z)$ in Fig. 2, was estimated based on experiments with three human subjects and a KEMAR mannequin [8]. In order to identify the acoustic feedback path, white noise was sent to the hearing-aid receiver while the forward path of the hearing-aid was disconnected. The signals sent to the receiver and those received at the microphone were simultaneously recorded on a DAT. Using these measurements, a 15-pole/14-zero linear model of the acoustic feedback path was determined using the Steiglitz-McBride algorithm [9]. The feedback path was modeled under both static and time-varying conditions. For the purposes of the analysis and simulations, the first 101 samples (12.625 ms with a sampling rate of 8 KHz) of the model's impulse response, shown in Fig. 4, were used to construct a 100th order FIR model of the feedback path. An additional impulse response, shown in Fig. 5, was obtained from other measurements performed at the House Ear Institute, Los Angeles.

It is important to note that this work assumes that the adaptive filter is capable of approximating the feedback path with no residual error, i.e., the transversal adaptive filter has the same order of the feedback path, and is assumed to be FIR. In actual implementations, however, the feedback path transfer function may have an impulse response of higher order than that of the adaptive filter. In that case, the estimation process will result in a residual error since only some samples of the feedback path

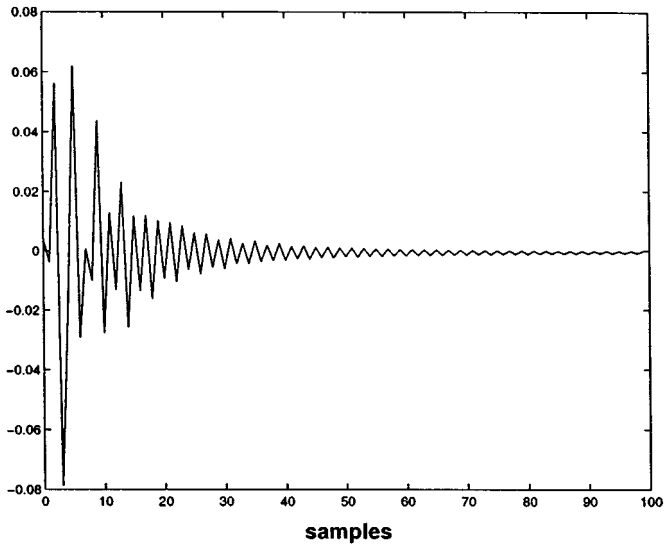

Fig. 4. Impulse response of a hearing-aid feedback path for a human subject.

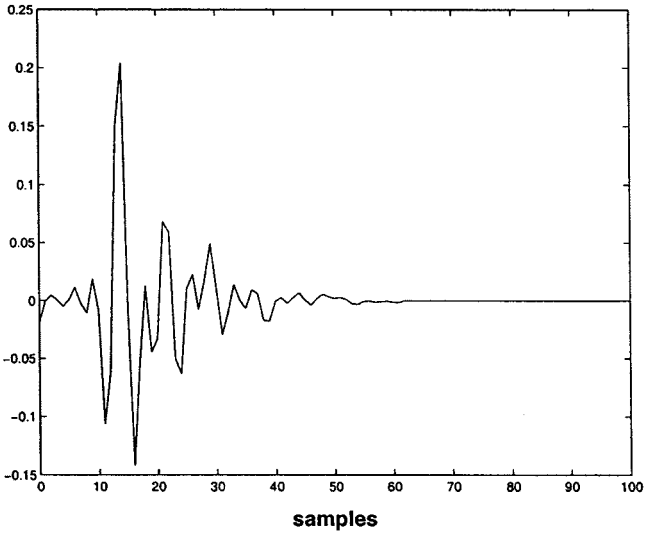

Fig. 5. Impulse response of an alternate feedback path.

impulse response will be estimated. In this paper, it is assumed that the adaptive filter and the feedback path are both FIR and of the same order (N).

III. Steady-State Analysis Using Continuous Adaptation

This section will address the performance of Wiener filter estimates for a continuous-time adaptation system for hearing aids. The purpose is to determine the steady-state behavior of adaptive filters that approximate the Wiener solution, such as the LMS algorithm.

A. Bias in the Wiener Estimate

A Wiener filter estimates a system transfer function $H(z)$ given the input signal to the system $s(n)$ and a corrupted system output signal $d(n)$ as illustrated in Fig. 6. The corrupted signal is assumed to be the convolution between the system impulse

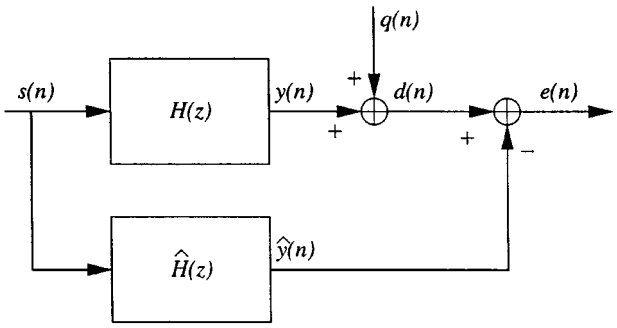

Fig. 6. Wiener estimate of a linear system $H(z)$.

response $h(n)$ and the input signal $s(n)$ added to a noise component $q(n)$. It can be written as

$$d(n) = s(n) * h(n) + q(n). \tag{1}$$

In most cases, $q(n)$ is assumed to be white noise. The discrete-time FIR Wiener filter estimate [7] for $H(z)$ is a vector $\hat{\mathbf{h}}$ which represnts the impulse response coefficients and is given by

$$\hat{\mathbf{h}} = \mathbf{R}_{ss}^{-1}\mathbf{r}_{sd} \tag{2}$$

where

$$\mathbf{R}_{ss} \triangleq E\{\mathbf{s}(n)\mathbf{s}^T(n)\} \tag{3}$$

$$\mathbf{r}_{sd} \triangleq E\{\mathbf{s}(n)\, d(n)\} \tag{4}$$

$$\mathbf{s}(n) \triangleq [s(n) \quad s(n-1) \quad \cdots \quad s(n-N)]^T \tag{5}$$

and N is the order of the Wiener estimate.

Now consider the case where the interference signal $q(n)$ is derived from the input signal $s(n)$ by a linear system. It is easy to prove that (2) will not lead to a proper estimate of the impulse response of $H(z)$. The Wiener estimate impulse response vector $\hat{\mathbf{h}}$ deviates from the impulse response of $H(z)$ by

$$\boxed{\varepsilon = \mathbf{R}_{ss}^{-1}\mathbf{r}_{sq}} \tag{6}$$

where ε is defined as

$$\varepsilon = \hat{\mathbf{h}} - \mathbf{h} \tag{7}$$

and $\mathbf{h}$ is a vector representing the impulse response of $H(z)$.

B. Application to a Feedback Reduction System

In this section, expressions for the bias are derived for the cases of delayed forward or cancellation paths in the hearing-aid plant. A delay is used to decorrelate the input and output signals in the continuous-adaptation feedback reduction plant for hearing aids. Superscripts f and c will be used to indicate when a delay is used in the forward and cancellation paths, respectively. All vectors are assumed to have the Wiener filter length ($N+1$ taps—Nth-order estimate) except where indicated with subscripts.

In the analysis, the bias in the feedback reduction system will be defined as

$$\varepsilon = \mathbf{w} - \mathbf{f} \tag{8}$$

where $\mathbf{w}$ is a vector representing the Wiener estimate for a hearing aid plant based on the signals $x(n)$ and $d(n)$ and $\mathbf{f}$ is a vector representing the feedback path impulse response (see Fig. 3).

1) Bias with a Delayed Forward Path: In the hearing aid plant shown in Fig. 3(b), it can be seen that the response signal $d(n)$ is

$$d(n) = y(n) + x(n) \tag{9}$$

where $y(n)$ is the output of the feedback path. By using (6) and (9), it follows that the bias in the Wiener estimate of the feedback path $F(z)$ is

$$\boxed{\varepsilon^f = \mathbf{R}_{ss}^{-1}\mathbf{r}_1^f} \tag{10}$$

where

$$\mathbf{r}_1^f = E\{\mathbf{s}(n)x(n)\}. \tag{11}$$

2) Bias with a Delayed Cancellation Path: In the case of the hearing aid plant shown in Fig. 3(a), the input signal to the adaptive filter is delayed by Δ samples. In this case, the Wiener filter will estimate the last $N+1$ terms of the impulse response, since the first Δ samples of the impulse response are implicitly approximated by zeroes.

The feedback path shown in Fig. 3(a) is assumed to be FIR and with a transfer function $F(z)$. It is also assumed that it can be divided into two components

$$F_1(z) = \mathbf{f}_{1,\Delta}^T\mathbf{t}_\Delta(z^{-1}) \tag{12}$$

$$F_2(z) = \mathbf{f}_2^T\mathbf{t}(z^{-1}) \tag{13}$$

where $\mathbf{f}_{1,\Delta}$ is a vector representing the first Δ samples of the impulse response, $\mathbf{f}_2$ is a vector with $N+1$ samples, and $\mathbf{t}_\Delta(z)$ and $\mathbf{t}(z)$ are defined as

$$\mathbf{t}_\Delta(z) \triangleq [1 \quad z \quad \cdots \quad z^{\Delta-1}]^T \tag{14}$$

$$\mathbf{t}(z) \triangleq [1 \quad z \quad \cdots \quad z^{N}]^T. \tag{15}$$

The feedback path transfer function can thus be written as a function of $F_1(z)$ and $F_2(z)$ as follows:

$$F(z) = F_1(z) + z^{-\Delta}F_2(z). \tag{16}$$

Consequently, the feedback path output signal $y(n)$ can be divided into two components

$$y(n) = y_1(n) + y_2(n) \tag{17}$$

where

$$y_1(n) \triangleq \mathbf{f}_{1,\Delta}^T\mathbf{s}_\Delta(n) \tag{18}$$

$$y_2(n) \triangleq \mathbf{f}_2^T\mathbf{s}(n). \tag{19}$$

This is illustrated in Fig. 7. Note that Figs. 7 and 3(a) represent the same system. The signal $d(n)$ can thus be written as

$$d(n) = y_1(n) + y_2(n) + x(n). \tag{20}$$

Considering that the adaptive filter will only be able to approximate $F_2(z)$, it is clear that the bias will contain two components in this case: the first is due to the transfer function between $x(n)$ and $s(n)$, and the second bias term is due to the output of $F_1(z)$. The bias can then be written as

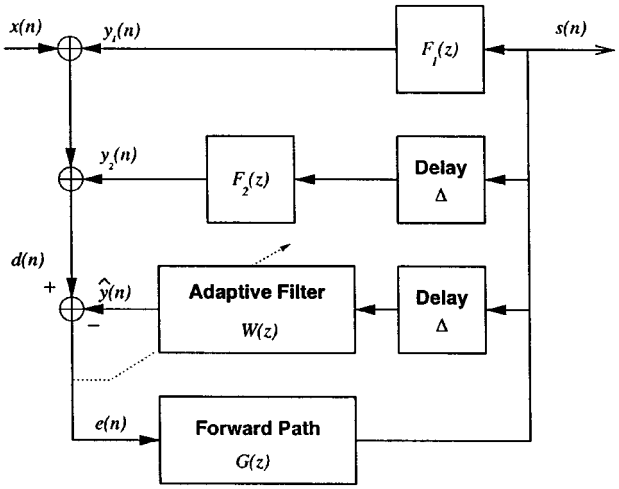

Fig. 7. Model of a hearing aid plant with a delay in the cancellation path and with the feedback path divided into two components.

$$\varepsilon_2^c = \mathbf{R}_{ss}^{-1}\mathbf{r}_1^c + \mathbf{R}_{ss}^{-1}\mathbf{r}_2^c \tag{21}$$

where

$$\mathbf{r}_1^c \triangleq E\{\mathbf{s}(n-\Delta)x(n)\} = E\{\mathbf{s}(n)x(n+\Delta)\} \tag{22}$$

$$\mathbf{r}_2^c \triangleq E\{\mathbf{s}(n-\Delta)y_1(n)\} = E\left\{\mathbf{s}(n)\mathbf{s}_\Delta^T(n+\Delta)\right\}\mathbf{f}_{1,\Delta} \tag{23}$$

Note that ε_2^c in (21) gives the last $N+1$ entries of the bias vector. There is, however, another term in the bias vector due to approximating the first Δ samples of $F(z)$ with zeroes. This term of the bias can be written as

$$\varepsilon_{1,\Delta}^c = \mathbf{0} - \mathbf{f}_{1,\Delta} = -\mathbf{f}_{1,\Delta}. \tag{24}$$

Thus, the total bias is equal to

$$\boxed{\varepsilon^c = \begin{bmatrix} \varepsilon_{1,\Delta}^c \\ \varepsilon_2^c \end{bmatrix} = \begin{bmatrix} -\mathbf{f}_{1,\Delta} \\ \mathbf{R}_{ss}^{-1}\mathbf{r}_1^c + \mathbf{R}_{ss}^{-1}\mathbf{r}_2^c \end{bmatrix}.} \tag{25}$$

C. Steady-State Performance

Simulations were carried out to verify that the adaptive filter leads to a biased solution when correlated hearing-aid input signals are used. In addition, simulations were performed to compare the steady-state performance of the feedback reduction system when delays are used in the forward and cancellation paths. In the simulations, a feedback path with an impulse response shown in Fig. 4 was used. The inputs were white gaussian noise and speech-shaped noise with a low-pass magnitude transfer function [10].

The performance criterion used to estimate the extent to which the adaptive filter approximates the feedback path impulse response is misalignment, defined by

$$\|\varepsilon(n)\| = \|E\{\mathbf{w}(n) - \mathbf{f}\}\|. \tag{26}$$

This metric is the norm of the difference between the adaptive filter estimate vector $\mathbf{w}(n)$ and the feedback path coefficients vector $\mathbf{f}$. In steady state, the metric is the norm of the bias in the adaptive filter estimate.

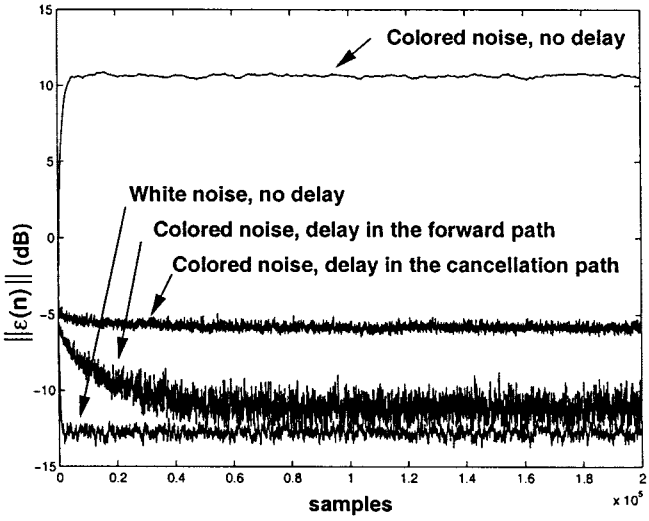

Fig. 8. Misalignment when the input is white or speech-shaped noise. Two cases were considered with speech-shaped noise: no delay, and a delay of 10 samples in either the forward or cancellation paths. The forward gain was $G_0 = 3$. The feedback path was modeled with the impulse response in Fig. 4.

Fig. 8 shows the misalignment of the NLMS (normalized LMS [7]) adaptive filter with convergence factor $\mu = 0.1$ and order $N = 100$ for both white noise and speech-shaped noise input signals, with and without a delay. A total of 5 experiments were run to simulate the ensemble average. The equations for the NLMS algorithm are

$$e(n) = d(n) - \mathbf{w}^T(n)\tilde{\mathbf{s}}(n) \tag{27}$$

$$\mathbf{w}(n+1) = \mathbf{w}(n) + \frac{\mu}{||\tilde{\mathbf{s}}(n)||}\tilde{\mathbf{s}}(n)e(n) \tag{28}$$

where $\mathbf{w}(n) = [w_0(n) \ \cdots \ w_N(n)]^T$ is a vector of order N containing the instantaneous taps update, $\tilde{\mathbf{s}}(n) = [\tilde{s}(n) \ \cdots \ \tilde{s}(n-N)]^T$ is a vector of order N with input samples of the adaptive filter, $e(n)$ is the *a priori* error signal and $d(n)$ is the desired response signal. It is important to note that $\tilde{s}(n) = s(n)$ for a delayed forward path and $\tilde{s}(n) = s(n-\Delta)$ for a delayed cancellation path (see Fig. 3).

As expected, when a white noise input signal is used, the hearing-aid input and output signals are reasonably well decorrelated, thus reducing the adaptive filter bias. When the input signal is correlated noise, however, a bias results, as illustrated in Fig. 8.

Fig. 8 also shows that if the input is correlated noise and a delay is included in the forward path, performance improves by 20 dB resulting in $||\varepsilon(n)|| \leq -10$ dB in steady state. The delay used was 10 samples at 8 kHz. When the same delay is used in the cancellation path, the adaptive filter also converges, but with a higher bias. This can be explained by the fact that a delayed cancellation path results in approximating the first Δ samples of the feedback impulse response with zeros, an inappropriate approximation for the feedback path used here, thus causing a higher bias.

The results can also be explained by observing that the bias vector for the delayed cancellation-path has two terms (ε_2^c and $\varepsilon_{1,\Delta}^c$). The first term (ε_2^c) is given by (21), while the second term ($\varepsilon_{1,\Delta}^c$) is equal to $-\mathbf{f}_{1,\Delta}$, the first Δ samples of the impulse response. Thus, the minimum bias will be equal to $-\mathbf{f}_{1,\Delta}$, and will be attained only if the adaptive filter is capable of perfectly estimating the feedback path ($\varepsilon_2^c = \mathbf{0}$).

In the next section, an analytical study will show that the bias in the case of a delay in the forward path is independent of the feedback path impulse response, and this result is in contrast with the case where a delay is placed in the cancellation path. It will also be shown that it is possible to predict the value of the bias in the Wiener solution for both cases. Determining the value of the bias in the adaptive filter's steady-state solution is important for calculating the overall system gain margins with guaranteed stability.

IV. Effect of Decorrelation Delay

Determining quantitative relations for the bias as a function of the input signal statistics, the delay (Δ), and the forward path gain (G_0) is complicated for arbitrary signals. This section is an analytical study of the case where the input is a colored sequence derived from an M-pole filtered white noise (Markov process). The model for the forward path was described previously [4] and assumes that the error signal $e(n)$ is amplified by a constant gain G_0 and delayed so that $G(z) = G_0 z^{-1}$. The extension to a more general $G(z)$ is straightforward and includes a matrix multiplication operation in most of the formulae.

A. Bias Reduction by Use of a Delayed Forward Path

In the case where the forward path $G(z)$ is modeled as $G(z) = G_0 z^{-1}$, it is possible to express the input to the adaptive filter $s(n)$ as a function of the error signal as

$$s(n) = G_0 e(n - \Delta - 1). \tag{29}$$

Thus, (10) and (11) can be rewritten as a function of the cross-correlation sequence $r_{ex}^f(m)$ and the autocorrelation matrix $\mathbf{R}_{ee}^f$ as follows:

$$\varepsilon^f = \frac{1}{G_0^2}\left[\mathbf{R}_{ee}^f\right]^{-1}\mathbf{r}_1^f \tag{30}$$

$$\mathbf{r}_1^f = G_0 E\{\mathbf{e}(n-\Delta-1)x(n)\} = G_0\mathbf{r}_{ex}^f(\Delta+1). \tag{31}$$

where

$$\mathbf{e}(n-\Delta-1) = [e(n-\Delta-1) \quad e(n-\Delta-2) \ \cdots \ e(n-\Delta-N-1)]^T. \tag{32}$$

Hence, to compute the elements of ε^f, it is necessary to calculate the cross-correlation sequence $r_{ex}(m)$ and the autocorrelation sequence $r_{ee}(m)$. The equations for the cross-correlation and autocorrelation sequences $r_{ex}(m)$ and $r_{ee}(n)$ are derived in Appendix I for the case where the input to the hearing aid is a Markov process. It is shown that $r_{ee}(m)$ and $r_{ex}(m)$ are functions of ε^f. These relations result in a set of nonlinear equations that are not easily solved analytically. However, it is possible to

compute ε^f from these equations by using the following iterative procedure:

1- Set ε^f = initial guess
2- Calculate $r^f_{\acute{e}x}(m)$ using (42)
3- Calculate $r^f_{\acute{e}\acute{e}}(m)$ using (47)
4- Calculate $\mathbf{r}^f_1$ using (31)
5- Calculate $\hat{\varepsilon}^f$ using (30)
6- If $\|\hat{\varepsilon}^f - \varepsilon^f\| \leq \delta_{\min}\|\hat{\varepsilon}^f\|$: STOP
7- Otherwise $\varepsilon^f \leftarrow \hat{\varepsilon}^f$: go to step 2.

In the above procedure, $\hat{\varepsilon}^f$ is the iterative estimate of ε^f, $\delta_{\min}$ is the minimum normalized precision for the algorithm's convergence—a typical value is 10^{-2}. One possible way to choose the initial guess is by setting it equal to zero (or to a very small value) and choosing a sufficiently large value for Δ, say $\Delta = \Delta_{\text{in}}$. Once the algorithm converges to a value of ε^f, this value can then be used as an initial guess for the case where $\Delta = \Delta_{\text{in}} - 1$. The resulting estimate of ε^f can be used as an initial estimate for $\Delta = \Delta_{\text{in}} - 2$, and so on, until $\Delta = 0$.

Although there is no guarantee that numerical methods for solving sets of nonlinear equations will converge to the desired solution, the above procedure converges to the desired solution in most cases. As will be shown in the next section, the above procedure usually converges to the desired solution when the forward path delay is greater than six samples at a sampling rate of 8 KHz.

1) Numerical Results: Simulations were performed to verify the outlined numerical method for computing $\|\varepsilon^f\|$. In all simulations, a 5 million point data sequence and an adaptive filter order of 20 were used with the NLMS algorithm. A small convergence factor of $\mu = 0.01$ was used to reduce the effect of excess mean-squared error in the simulations. The feedback path was modeled with the first 21 samples of the impulse response shown in Fig. 4. The input was a 12th order Markov process derived from a white Gaussian input that models speech-shaped noise [10]. Plots illustrating the theoretical and experimental results are shown in Fig. 9. The solid curve represents simulation values while the dashed curve represents predicted values. For $\Delta < 7$ samples, the predicted curve is discontinued because the numerical procedure converged to a solution that did not agree with the simulation results. The number of iterations for the described method range from 5–10 iterations for high values of Δ (around 40) to 40–50 iterations for values of Δ around 10.

For $\Delta > 14$ samples, there is a difference between the two curves in Fig. 9. This can be explained by practical limitations. A total number of points greater than 5 million and a smaller convergence factor would be necessary to achieve a better match between the two curves with a sufficiently low excess mean square error [7].

2) Results for a One-Tap Adaptive Filter and a First-Order Markov Process Input: Although the case of a single tap and a single-pole input is not as general as the one addressed in the previous section, it allows us to derive an expression for the bias as a function of the pole, the forward gain G_0, and delay in the forward path, Δ. The derivations are shown in Appendix II. The equation for the bias in this case is

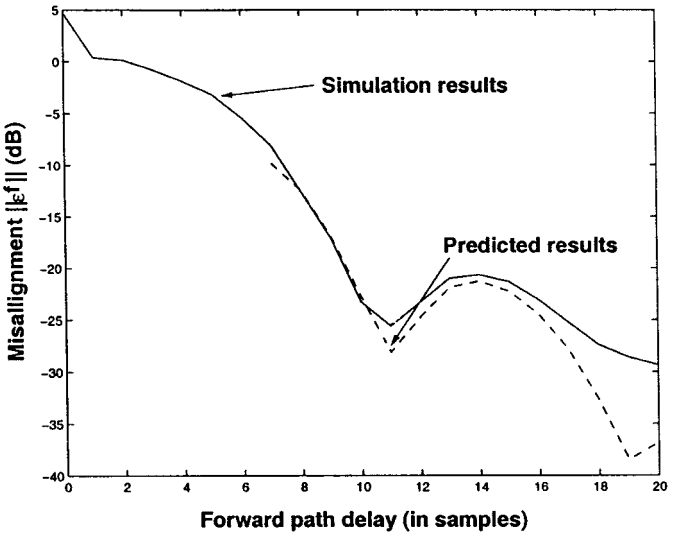

Fig. 9. Steady-state misalignment $\|\varepsilon^f\|$ as a function of forward path delay (in samples) for $G_0 = 2$. Continuous lines represent simulation results and dashed lines, predicted values. The input was speech-shaped noise. The feedback path was modeled with the first 21 samples of the impulse response in Fig. 4.

$$\boxed{\varepsilon^f_0 = \frac{\rho^{\Delta+1}}{G_0}} \tag{33}$$

where ρ is the Markov process constant.

Computer simulations were performed to evaluate the analytical estimate of the adaptive filter convergence error for a one tap adaptive filter. In the simulations, the gain G_0 was set to 2 and 4, the Markov process constant ρ was set to 0.9, and delay (Δ) was between 0 and 40 samples. The NLMS algorithm was used with $\mu = 0.01$. The feedback path was modeled with the first sample of the impulse response shown in Fig. 4 $(F(z) = 0.0778)$. Simulated and predicted results [from (33)] are shown in Fig. 10. Again, solid lines represent simulated values and the dashed lines represent values obtained with (33).

From Fig. 10, it can be seen that the magnitude of the taps' deviation is reduced with increasing delay (Δ) and for higher gains. Simulations in Section V will show that these results hold for more general cases.

B. Bias Reduction by Use of a Delayed Cancellation Path

In the delayed cancellation path case, the second term of the bias in the adaptive filter estimate (21), is reproduced below as a function of $\mathbf{R}^c_{\acute{e}\acute{e}}$ and $r^c_{\acute{e}x}(m)$, the autocorrelation matrix for $e(n)$ and the cross-correlation between $x(n)$ and $e(n)$, respectively.

$$\varepsilon^c_2 = \frac{1}{G_0^2}\left[\mathbf{R}^c_{\acute{e}\acute{e}}\right]^{-1}\mathbf{r}^c_1 + \frac{1}{G_0^2}\left[\mathbf{R}^c_{\acute{e}\acute{e}}\right]^{-1}\mathbf{r}^c_2 \tag{34}$$

$$\mathbf{r}^c_1 \triangleq G_0 E\{\mathbf{e}(n-\Delta-1)x(n)\} = G_0 E\left\{\mathbf{r}^c_{\acute{e}x}(m)\right\} \tag{35}$$

$$\begin{aligned}\mathbf{r}^c_2 &\triangleq G_0 E\{\mathbf{e}(n-\Delta-1)y_1(n)\}\\ &= G_0^2 E\left\{\mathbf{e}(n)\mathbf{e}^T_\Delta(n+\Delta)\right\}\mathbf{f}_{1,\Delta}.\end{aligned} \tag{36}$$

Hence, to compute the elements of ε^c_2, it is necessary to calculate the cross-correlation sequence $r^c_{\acute{e}x}(m)$ and the autocorrelation sequence $r^c_{\acute{e}\acute{e}}(m)$. The equations for the sequences $r^c_{\acute{e}x}(m)$ and $r^c_{\acute{e}\acute{e}}(n)$ are derived in Appendix I for the case where the

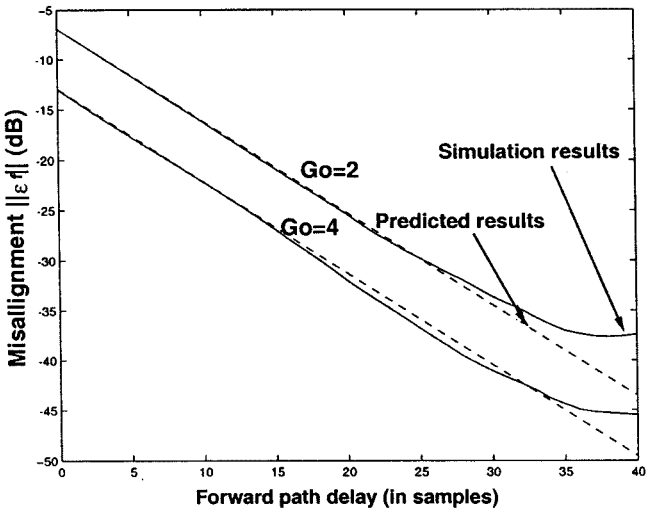

Fig. 10. Steady-state misalignment $||\varepsilon_0^f||$ as a function of forward path delay (in samples) for $G_0 = 2$ and $G_0 = 4$. Continuous lines represent simulation results and dashed lines represent predicted values. The input was a 1st order Markov Process. The feedback path was modeled with the first sample of the impulse response shown in Fig. 4 ($F(z) = 0.0778$).

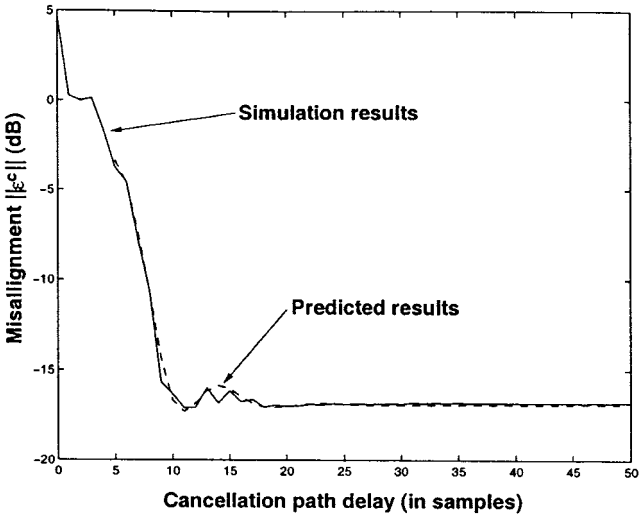

Fig. 11. Steady-state misalignment $||\varepsilon^c||$ as a function of cancellation path delay (in samples) for $G_0 = 2$. Continuous lines represent simulation results and dashed lines, predicted values. The input was speech-shaped noise (12th order Markov Process). The feedback path was modeled with the first 21 samples of the impulse response in Fig. 4.

input to the hearing aid is a Markov process. Both $r_{ee}^c(m)$ and $r_{ex}^c(m)$ are functions of ε_2^c (see Appendix I), and these relations result in a set of nonlinear equations that are not easily solved analytically. It is possible to compute ε_2^c from these equations by using an iterative procedure similar to the one described in the previous section. The numerical procedure is as follows:

1- Set $\varepsilon_2^c =$ initial guess
2- Calculate $r_{ex}^c(m)$ using (51)
3- Calculate $r_{ee}^c(m)$ using (53)
4- Calculate $\mathbf{r}_1^c$ using (35) and $\mathbf{r}_2^c$ using (36)
5- Calculate $\hat{\varepsilon}_2^c$ using (34)
6- If $||\hat{\varepsilon}_2^c - \varepsilon_2^c|| \leq \delta_{\min}||\hat{\varepsilon}_2^c||$: STOP
7- Otherwise $\varepsilon_2^c \leftarrow \hat{\varepsilon}_2^c$: go to step 2.

The outlined procedure converges to the desired solution in most cases, as will be shown in the next section. The initial guess can be chosen in a way similar to that described for a delay in the forward path. The total bias is given by (25).

1) Numerical Results: Simulations were performed to verify the outlined numerical method for computing $||\varepsilon^c||$. In all simulations, 5 million points and an adaptive filter order of 20 were used with the NLMS algorithm. A small convergence factor of $\mu = 0.01$ was used to reduce the effect of excess mean-squared error in the simulations. The feedback path was modeled with the first 21 samples of the impulse reponse shown in Fig. 4. The input was a 12th-order Markov sequence derived from a white Gaussian input that models speech-shaped noise. Theoretical and simulated curves are shown in Fig. 11. The continuous curve represents simulation values and the dashed curve represents predicted values. It can be seen that for $\Delta < 7$ samples, the theoretical curve is discontinued because the numerical procedure converged to a solution that did not agree with the simulation results.

V. Simulations

In the previous section, analytical predictions of the bias were verified through simulations. In this section, we extend the simulations to include a different feedback path, a wider range of gains, and speech-shaped noise as the input. These simulations allow a comparison of systems with delayed forward and cancellation paths. We also discuss other properties of the adaptation schemes.

Computer simulations were conducted to evaluate the effectiveness of the NLMS algorithm in estimating the feedback path when a delay is used to decorrelate the hearing-aid input $x(n)$ and output signals $s(n)$. The model of the acoustic feedback path used a 100th order FIR linear filter with impulse responses shown in Figs. 4 and 5. A constant gain G_0 and a single delay were used to model the forward path transfer function $G(z)$ so that $G(z) = G_0 z^{-1}$. No frequency-shaping filter or automatic gain control (AGC) was used in the forward path model. The simulations were performed using speech-shaped noise with variance of 65 dB as the hearing-aid input signal $x(n)$. Speech-shaped noise was generated by passing white Gaussian noise through a 12-pole frequency shaping filter. A sampling rate of 8 KHz was used. The NLMS algorithm [7] used a normalized convergence factor $\mu = 0.1$ and order $N = 100$.

A. Steady-State Performance as a Function of Delay

The objective of the simulations was to evaluate the steady-state performance of the adaptive filter for various delays. Figs. 12 and 13 show the average misalignment in the steady-state over a range of delays for four values of the forward path gain G_0 (2, 3, 7, and 12) where the feedback path impulse response is shown in Fig. 4. A total of 200 000 samples were used in each simulation. The average misalignment was obtained by averaging the norm of the difference vector $[||\mathbf{w}(n) - \mathbf{f}||]$ over the last 50 000 samples.

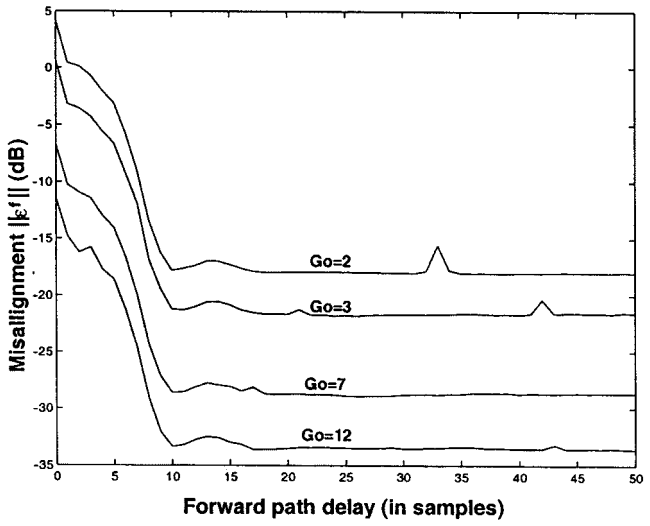

Fig. 12. Steady-state misalignment $||\varepsilon^f||$ vs. number of samples in the forward path delay for $G_0 = 2, 3, 7, 12$. The feedback path used is shown in Fig. 4. The input was speech-shaped noise.

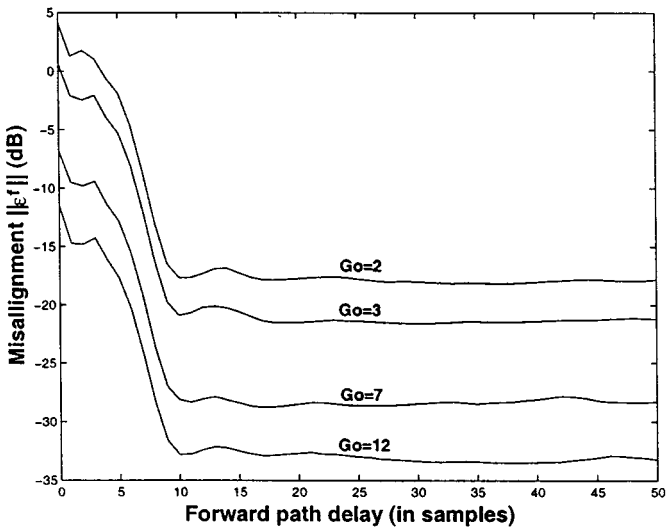

Fig. 14. Steady-state misalignment $||\varepsilon^f||$ versus number of samples in forward path delay for $G_0 = 2, 3, 7, 12$. The feedback path used is shown in Fig. 5. The input was speech-shaped noise.

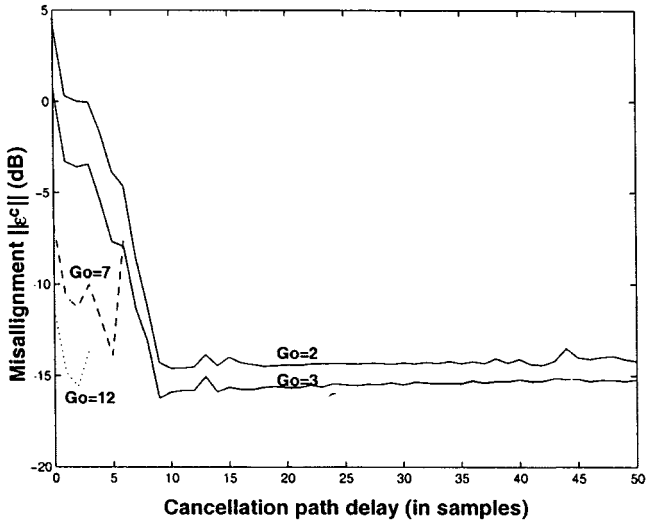

Fig. 13. Steady-state misalignment $||\varepsilon^c||$ vs. number of samples in the cancellation path delay for $G_0 = 2, 3, 7, 12$. The feedback path used is shown in Fig. 4. The input was speech-shaped noise.

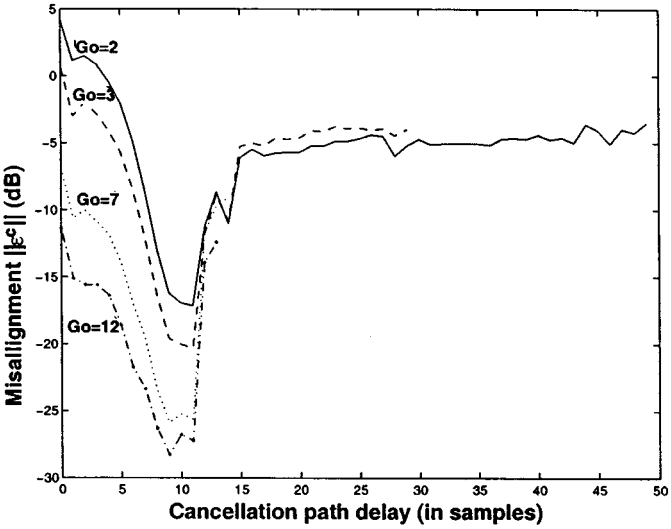

Fig. 15. Steady-state misalignment $||\varepsilon^c||$ versus number of samples in cancellation path delay for $G_0 = 2, 3, 7, 12$. The feedback path used is shown in Fig. 5. The input was speech-shaped noise.

Fig. 12 shows that the best steady-state misalignment is attained when the forward path delay is 10 samples (1.25 ms) or higher and that the adaptive filter is more accurate in estimating the acoustic feedback path impulse response when higher gains are used.

Fig. 13 shows the bias as a function of the delay in the cancellation path. The curves for $G_0 = 7$ and 12 are discontinuous because the adaptive filter is unstable with a delay greater than eight and four samples, respectively. The reason for the relatively poor performance in this case is that the use of a delay in the cancellation path will approximate the first Δ samples of the impulse response with zeros—an unreasonable approximation for the feedback path shown in Fig. 4.

To examine the behavior of the algorithms when a different feedback path is used, simulations were carried out for the cases where most of the feedback path impulse response energy is not concentrated in the first samples. The impulse response of a different feedback path is shown in Fig. 5; simulation results are shown in Figs. 14 and 15. Comparing Figs. 14 and 12, one notices that the magnitude of the bias vector is relatively independent of the feedback path when a delayed forward path is used. On the other hand, a comparison of Figs. 15 and 13 indicates that, for a delayed cancellation path, higher gains can be used only if the feedback path impulse response does not have most of its energy concentrated in the first samples. With the feedback path shown in Fig. 5, a delayed cancellation path allowed higher gains for a delay of 10–15 samples. A delay of more than 15 samples in the cancellation path made the adaptive filter unstable for high gains, due to the poor approximation of the samples 10–15 of the impulse response in Fig. 5.

B. Choice of Delay

The simulations discussed previously, illustrated in Figs. 12–15, clearly show that the smallest value of delay that

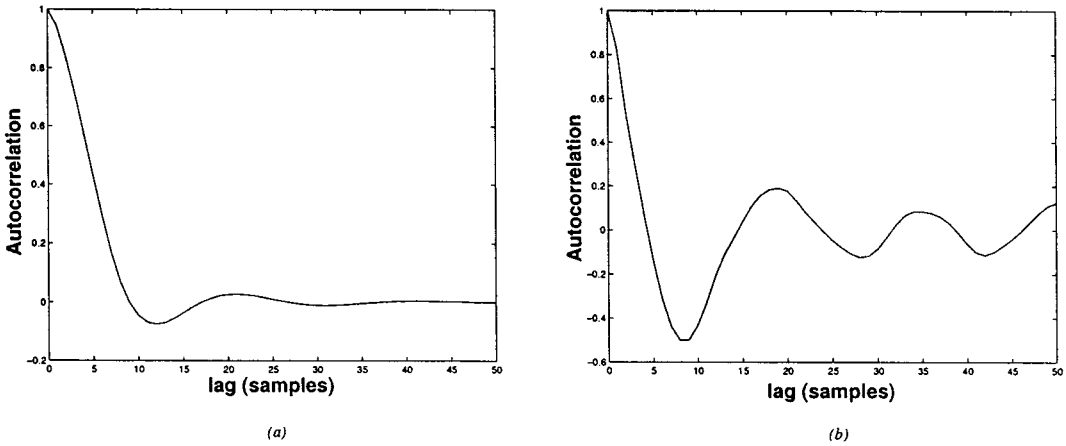

Fig. 16. (a) Autocorrelation sequence of speech-shaped noise (2^{19} samples). (b) Autocorrelation sequence of a sentence (31265 samples).

effectively reduces the bias is around 10 samples (1.25 ms); this value is the same as that chosen by Bustamante *et al.* [1] and Estermann and Kaelin [4] experimentally. This delay can also be justified by the autocorrelation sequence of the input signals. When the input is speech-shaped noise, its autocorrelation decays continuously until a lag of 10 samples (1.25 ms) [Fig. 16(a)], and it does not show a significant decrease with greater lags. When the input is a sentence with 31 265 samples, the autocorrelation shows a similar behavior [Fig. 16(b)].

C. Convergence Rate as a Function of Delay

The simulations in this section indicate that a delay in the forward and cancellation paths allows a reduction of the bias at the expense of a slower convergence rate. Comparing the curves in Fig. 8 it can be seen that the convergence of the NLMS algorithm is slower when delays are used. Previous works [11], [12] have acknowledged a reduction in convergence speed as a function of delays in the updates of the LMS algorithm.

D. Dependence of the Bias on the Feedback Path

As mentioned earlier, depending on the characteristics of the feedback path, a delay in the cancellation path might prevent the adaptive filter from converging. There is a clear dependency of the adaptive filter performance on the number of samples of delay in the cancellation path. Equations (51) and (52) in Appendix I show that the elements of the vectors $\mathbf{r}_1^c$, $\mathbf{r}_2^c$ and $\mathbf{R}_{ee}^c$ are dependent on $\mathbf{f}_{1,\Delta}$, thus explicitly showing that the bias in this case is a function of the first Δ elements of the feedback path impulse response. This result is in contrast with the delayed forward path case where the bias is independent of the feedback path characteristics. Equations (42) and (43) show that the elements of $\mathbf{r}_1^f$ and $\mathbf{R}_{ee}^f$ are independent of the feedback path coefficients. Finally, the simulations shown in Figs. 12 –15 indicate that when delays are used in the forward path, the bias curves have the same shape when different feedback paths are used, while the same result does not hold for a delayed cancellation path.

VI. Conclusion

In this paper, it was shown that the closed-loop plant used in continuous-time feedback reduction systems for hearing aids results in biased estimations of the feedback path when correlated input signals are used. Analysis in the case of an Mth-order Markov process input signal was presented, and equations that allow prediction of the bias were derived. The analysis was extended to the cases where the forward path or the cancellation path are delayed to decorrelate the error signal and the input signal to the adaptive filter. The analysis justifies the role of delay, which had been proposed previously in the forward and cancellation paths of continuous adaptation systems for hearing aids [1], [4], and illustrates how delay decreases the bias in the adaptive filter's estimate. The analysis allows the prediction of the magnitude of the bias, while previous works relied on subjective evaluation for determining the steady-state performance of feedback reduction systems.

Simulations and theoretical analysis indicate that a reduction of more than 15 dB in the misalignment can be obtained when the input signal is speech-shaped noise and a delay is used either in the forward or cancellation paths. It was also shown that a better approximation is obtained as the forward path gain increases.

If a delay is used in the cancellation path, the adaptive filter might not be able to satisfactorily approximate the feedback path, causing the system to become unstable for high values of the forward gain. This result can be explained by observing that when a delay is used in the cancellation path, it approximates the first Δ samples of the impulse response with zeros, causing the bias to be dependent on initial values of the impulse response. It is important to note that a delay in the feedback path may be introduced by sigma-delta A/D and D/A converters. In this case, a delayed cancellation path that properly matches the delay introduced by the converters may have the advantage of permitting a lower order adaptive filter.

The derived equations show that the bias is independent of the feedback path characteristics if a delay is introduced in the forward path. Simulations and theoretical curves with a delay in the forward path have shown that the magnitude of bias does not decrease significantly with a delay greater than 10 samples (1.25 ms for a sampling rate of 8 KHz). The theoretical analysis also showed that the bias reduction in the case of a delay in the forward path is not limited by the feedback path characteristics, unlike the delayed cancellation path case. This perhaps explains

why Estermann and Kaelin [4] obtained a higher increase in the critical gain of a hearing aid (20 dB) by using a delay in the forward path than Bustamante *et al.* [1], who used a delay in the cancellation path (6–10 dB). For this reason, and due to the fact that the feedback path impulse response usually has most of the energy concentrated in the first samples, delay in the forward path is preferred over delay in the cancellation path to reduce the bias in the adaptive filter's estimate.

APPENDIX I
CALCULATION OF AUTOCORRELATIONS AND CROSS-CORRELATIONS FOR MARKOV INPUTS

A. Calculation of $r^f_{\acute{e}x}(m)$

Assuming that $x(n)$ is an Mth-order Markov Process with M poles at ρ_i, $i = 1, \ldots, M$, and derived from white Gaussian noise $v(n)$ with variance σ_v^2, the transfer function $H_{xv}(z)$ can be written as

$$H_{xv}(z) = \frac{X(z)}{V(z)} = \frac{1}{\prod_{i=1}^{M}(1-\rho_i z^{-1})}. \tag{37}$$

According to Fig. 3(b), it is possible to write an equation for $e(n)$ as a function of $\epsilon^f(n)$ and $x(n)$ as follows:

$$e(n) = d(n) - G_0 \epsilon^{fT}(n)\mathbf{x}(n-\Delta-1) \tag{38}$$

where $\epsilon^f(n) = \mathbf{w}(n) - \mathbf{f}$. Using the above relation it is possible to determine the transfer function $H^f_{\acute{e}x}(z)$

$$H^f_{\acute{e}x}(z) = \frac{E(z)}{X(z)} = \frac{1}{1 + G_0 \varepsilon^{fT}\mathbf{t}(z^{-1})z^{-\Delta-1}} \tag{39}$$

where $\mathbf{t}$ is defined in (15). In the above equation, it is assumed that an LMS-based adaptive filter with a sufficiently small convergence factor μ was used, so that in steady-state

$$\lim_{n\to\infty} \epsilon^f(n) \approx \lim_{n\to\infty} E\{\epsilon^f(n)\} \triangleq \varepsilon^f \tag{40}$$

where ε^f is given by (10).

It is now possible to compute $r^f_{xe}(m)$ by using the Residue Theorem [13], and assuming that the transfer function in (39) is stable (poles inside the unit circle). For $m \geq 0$ the result is

$$r^f_{\acute{e}x}(m) = \mathcal{Z}^{-1}\left[\sigma_v^2 H_{xv}(z)H_{xv}(z^{-1})H^f_{\acute{e}x}(z)\right] \tag{41}$$

$$= \sigma_v^2 \sum_{i=1}^{M} \frac{\rho_i^{M-1}}{\prod_{\substack{j=1\\ i\neq j}}^{M}(\rho_i - \rho_j)} \frac{1}{\prod_{j=1}^{M}(1-\rho_i\rho_j)} \times \frac{1}{1 + G_0\varepsilon^{fT}\mathbf{t}(\rho_i)\rho_i^{\Delta+1}}\rho_i^m. \tag{42}$$

B. Calculation of $r^f_{\acute{e}\acute{e}}(m)$

The autocorrelation of $e^f(m)$ can be calculated using (38). It is possible to show that

$$r^f_{\acute{e}\acute{e}}(m) = r^f_{\acute{e}x}(m) - G_0\varepsilon^{fT}\mathbf{r}^f_{\acute{e}\acute{e}}(m-\Delta-1) \tag{43}$$

where $\mathbf{r}^f_{\acute{e}\acute{e}}(m-\Delta-1) = [r^f_{\acute{e}\acute{e}}(m-\Delta-1)\ r^f_{\acute{e}\acute{e}}(m-\Delta-2)\ \cdots\ r^f_{\acute{e}\acute{e}}(m-\Delta-N-1)]^T$.

Equation (43) can be rewritten as

$$r^f_{\acute{e}\acute{e}}(m) = r^f_{\acute{e}x}(m) - G_0\sum_{i=0}^{N}\varepsilon_i^f\, r^f_{\acute{e}\acute{e}}(|m-\Delta-i-1|). \tag{44}$$

The above equation can be rewritten in matrix form for $m = 0, \ldots, \Delta+1+N$

$$\begin{bmatrix} r^f_{\acute{e}\acute{e}}(0) \\ \vdots \\ r^f_{\acute{e}\acute{e}}(\Delta+1+N)\end{bmatrix} = \begin{bmatrix} r^f_{\acute{e}x}(0) \\ \vdots \\ r^f_{\acute{e}x}(\Delta+1+N)\end{bmatrix} - G_0\mathbf{K}^f\begin{bmatrix} r^f_{\acute{e}\acute{e}}(0) \\ \vdots \\ r^f_{\acute{e}\acute{e}}(\Delta+1+N)\end{bmatrix} \tag{45}$$

where $\mathbf{K}^f$ is a matrix with elements $k^f_{m,j}$ defined by

$$k^f_{m,j} = \varepsilon^f_{m-\Delta-1-j} + \varepsilon^f_{m-\Delta-1+j} \tag{46}$$

where it is assumed that $\varepsilon_i^f = 0$ for $i < 0$ or $i > N$. Equation (45) can be solved for determining $r^f_{\acute{e}\acute{e}}(m)$ as a function of $r^f_{\acute{e}x}(m)$ as follows:

$$\begin{bmatrix} r^f_{\acute{e}\acute{e}}(0) \\ \vdots \\ r^f_{\acute{e}\acute{e}}(\Delta+1+N)\end{bmatrix} = [G_0\mathbf{K}^f + \mathbf{I}]^{-1}\begin{bmatrix} r^f_{\acute{e}x}(0) \\ \vdots \\ r^f_{\acute{e}x}(\Delta+1+N)\end{bmatrix}. \tag{47}$$

For solving the above equation, it is necessary to first determine $r^f_{\acute{e}x}(m)$ and the elements of the matrix $\mathbf{K}^f$, which are functions of the bias vector elements ε_i^f.

C. Calculation of $r^c_{\acute{e}x}(m)$

According to Fig. 7, it is possible to express $e(n)$ as a function of $\epsilon_2^c(n)$ and $x(n)$ as follows:

$$e(n) = d(n) - G_0\epsilon_2^{cT}\mathbf{x}(n-\Delta-1) + G_0\mathbf{f}_1^T\mathbf{x}(n-1). \tag{48}$$

The transfer function $H^c_{\acute{e}x}(z)$ can now be determined as

$$H^c_{\acute{e}x}(z) = \frac{E(z)}{X(z)} = \frac{1}{1 - G_0\mathbf{f}^T_{1,\Delta}\mathbf{t}_\Delta(z^{-1})z^{-1} + G_0\varepsilon_2^{cT}\mathbf{t}(z^{-1})z^{-\Delta-1}} \tag{49}$$

where $\mathbf{t}_\Delta$ is defined in (14). In the above equation, assumption (40) applied to a delayed cancellation path was used. Now, the cross-correlation $r^c_{xe}(m)$ can be determined by using the inverse Z-Transform of $\Phi^c_{xe}(z)$ given by

$$\Phi^c_{xe}(z) = \sigma_v^2 H_{xv}(z)H_{xv}(z^{-1})H_{ex}(z). \tag{50}$$

To compute $r^c_{ex}(m)$ for $m \geq 0$ we note that $r^c_{ex}(m) = \mathcal{Z}^{-1}\{\Phi^c_{ex}(z)\} = \mathcal{Z}^{-1}\{\Phi^c_{xe}(z^{-1})\}$. Using the Residue Theorem [13], it is possible to calculate $r^c_{ex}(m)$

$$r^c_{ex}(m) = \sigma_v^2 \sum_{i=1}^{M} \frac{\rho_i^{M-1}}{\prod_{\substack{j=1\\ i\neq j}}^{M}(\rho_i - \rho_j)} \frac{1}{\prod_{j=1}^{M}(1-\rho_i\rho_j)} \times \frac{1}{1 - G_0\mathbf{f}^T_{1,\Delta}\mathbf{t}_\Delta(\rho_i)\rho_i + G_0\varepsilon_2^{cT}\mathbf{t}(\rho_i)\rho_i^{\Delta+1}}\rho_i^m. \tag{51}$$

D. Calculation of $r^c_{ee}(m)$

From (48) it is possible to calculate

$$r^c_{ee}(m) = r^c_{ex}(m) + G_0\mathbf{f}^T_{1,\Delta}\mathbf{r}^c_{ee,\Delta}(m-1) - G_0\varepsilon^{cT}_2\mathbf{r}^c_{ee}(m-\Delta-1). \quad (52)$$

In the above equation, $r^c_{ex}(m)$ is given by (51).

A relationship similar to (45) can be derived for the case where a delay is used in the cancellation path

$$\begin{bmatrix} r^c_{ee}(0) \\ \vdots \\ r^c_{ee}(\Delta+1+N) \end{bmatrix} = [G_0\mathbf{K}^c + \mathbf{I}]^{-1} \begin{bmatrix} r^c_{ex}(0) \\ \vdots \\ r^c_{ex}(\Delta+1+N) \end{bmatrix}. \quad (53)$$

The values of $r^c_{ex}(m)$ can be calculated from (51). The matrix $\mathbf{K}^c$ has elements $k^c_{m,j}$ defined by

$$k^c_{m,j} = \varepsilon^c_{m-\Delta-1-j} + \varepsilon^c_{m-\Delta-1+j} + f_{1,m-1-j} + f_{1,m-1+j} \quad (54)$$

where it was assumed that $\varepsilon^c_i = 0$ for $i < 0$ or $i > N$ and $f_{1,i} = 0$ for $i < 0$ and $i \geq \Delta$. For solving the above equation, it is necessary to first determine the elements of the matrix $\mathbf{K}^c$, that are a function of the bias vector ε^c_2.

APPENDIX II
BIAS FOR A SINGLE-POLE INPUT, SINGLE-TAP ADAPTIVE FILTER AND DELAYED FORWARD PATH

In the case of a single tap, (30) can be rewritten as

$$\varepsilon^f_0 = \frac{1}{G_0^2}\left[r^f_{ee}(0)\right]^{-1} r^f_{1,0} \quad (55)$$

where ε^f_0 is the first value of the vector $\varepsilon^f = E\{\epsilon^f\}$. $r^f_{1,0}$ can be calculated from (31) and (42) as follows

$$r^f_{1,0} = \frac{G_0\sigma_x^2\rho^{\Delta+1}}{1 + G_0\varepsilon^f_0\rho^{\Delta+1}}. \quad (56)$$

In the case of a single tap, (43) implies that

$$r^f_{ee}(0) = r^f_{xe}(0) = \frac{\sigma_x^2}{1 + G_0\varepsilon^f_0\rho^{\Delta+1}}. \quad (57)$$

Equation (55) can then be solved, and ε^f_0 can be calculated as follows

$$\varepsilon^f_0 = \frac{\rho^{\Delta+1}}{G_0}. \quad (58)$$

ACKNOWLEDGMENT

The authors would like to thank Dr. D. Morgan and the anonymous reviewers for their helpful suggestions. They are indebted to Dr. S. Soli of the House Ear Institute for his help in providing measurements of the feedback path and for many insightful comments.

REFERENCES

[1] D. Bustamante, T. Worrall, and M. Williamson, "Measurement of adaptive suppression of acoustic feedback in hearing aids," in *Proc. 1989 IEEE ICASSP*, 1989, pp. 2017–2020.
[2] J. Kates, "Feedback cancellation in hearing aids: Results from a computer simulation," *IEEE Trans. Signal Processing*, vol. 39, pp. 553–562, 1991.
[3] J. Maxwell and P. Zurek, "Reducing acoustic feedback in hearing aids," *IEEE Trans. Speech Audio Processing*, vol. 4, pp. 304–313, July 1995.
[4] P. Estermann and A. Kaelin, "Feedback cancellation in hearing aids: Results from using frequency-domain adaptive filters," in *Proc. 1994 IEEE ISCAS*, 1994, pp. 257–260.
[5] H. Joson, F. Asano, Y. Suzuki, and T. Sone, "Adaptive feedback cancellation with frequency compression for hearing aids," *J. Acoust. Soc. Amer.*, vol. 94, pp. 3248–3254, Dec. 1993.
[6] B. Widrow and S. Stearns, *Adaptive Signal Processing*. Englewood Cliffs, NJ: Prentice-Hall, 1985.
[7] S. Haykin, *Adaptive Filter Theory*. Upper Saddle River, NJ: Prentice-Hall, 1996.
[8] M. Siqueira, R. Speece, E. Petsalis, A. Alwan, S. Soli, and S. Gao, "Subband adaptive filtering applied to acoustic feedback reduction in hearing aids," in *Proc. 1996 Asilomar Conf. Signals, Systems, Computers*, Nov. 1996, pp. 778–782.
[9] P. Regalia, *Adaptive IIR Filtering in Signal Processing and Control*. New York: Dekker, 1994.
[10] D. Byrne and H. Dillon, *New Procedure for Selecting the Gain and Frequency Response of a Hearing Aid*: Ear and Hearing 7, The National Acoustic Laboratories, 1986.
[11] G. Long, F. Ling, and J. G. Proakis, "The LMS algorithm with delayed coefficient adaptation," *IEEE Trans. Acoust., Speech, Signal Processing*, vol. 37, pp. 1397–1405, Sept. 1989.
[12] ——, "Correction to 'the LMS algorithm with delayed coefficient adaptation'," *IEEE Trans. Acoust., Speech, Signal Processing*, vol. 40, pp. 230–232, Jan. 1992.
[13] A. Oppenheim and R. Schaffer, *Discrete-Time Signal Processing*. Englewood-Cliffs, NJ: Prentice-Hall, 1989.

Marcio G. Siqueira (M'00) received the B.Sc. and M.Sc. degrees in electrical engineering from the Federal University of Rio de Janeiro, Brazil, in 1990 and 1992, respectively, and the Ph.D. degree in electrical engineering from the University of California, Los Angeles, in 1998.

His research interests are digital filters, adaptive signal processing, hearing aids, speech and audio coding, and internet telephony. He has been with Philips Semiconductors since 1999.

Abeer A. H. Alwan (S'82–M'85) received the Ph.D. degree in electrical engineering from the Massachusetts Institute of Technology, Cambridge, in 1992.

Since then, she has been with the Electrical Engineering Department, University of California, Los Angeles (UCLA), as an Assistant Professor (1992–1996) and Associate Professor (1996–present). She established and directs the Speech Processing and Auditory Perception Laboratory at UCLA. Her research interests include modeling human speech production and perception mechanisms and applying these models to speech-processing applications.

Dr. Alwan is the recipient of the NSF Research Initiation Award (1993), the NIH FIRST Career Development Award (1994), the UCLA-TRW Excellence in Teaching Award (1994), the NSF Career Development Award (1995), and the Okawa Foundation Award in Telecommunications (1997). She is a member of Eta Kappa Nu, Sigma Xi, Tau Beta Pi, and the New York Academy of Sciences. She is an elected member of the IEEE Signal Processing Technical Committees on Audio and Electroacoustics and on Speech Processing. She was an elected member of the Acoustical Society of America Technical Committee on Speech Communication (1993–1999).